

## Contents

<b>1 Objective of Proposed Work</b>	<b>1</b>
<b>2 Fe and Fe/Ni Line Complex Ratios in Flares</b>	<b>2</b>
<b>3 Imaging Spectroscopy</b>	<b>9</b>
<b>4 Impact of Proposed Work</b>	<b>13</b>
<b>5 Relevance of Proposed Work to the NASA Programs/Objectives</b>	<b>14</b>
<b>6 Work Plan and Personnel</b>	<b>14</b>
<b>7 References</b>	<b>15</b>
<b>8 Biographical Sketch</b>	<b>17</b>
<b>9 Current and Pending Support</b>	<b>19</b>
<b>10 Budget Justification</b>	<b>20</b>

## Scientific/Technical/Management

### 1. Objective of Proposed Work

Solar flares emit a wide range of radiation extending from radio waves through  $\gamma$ -rays. The focus of this proposal will be the X-ray emission from high temperature plasmas in flares. We seek to use RHESSI data and data from other instruments (in particular, GOES and TRACE) to describe the thermal emission from solar flares. This will enable good estimates for the energy contained in the thermal flare plasma. This will also allow improved estimates for the nonthermal cutoff energy, and thus improved estimates of the energy in nonthermal electrons. In turn, good energy estimates provide information about the heating of plasma in flares and the acceleration of electrons. For example, one long-standing issue has been the determination of the fraction of total energy in flare emission that can be attributed to accelerated electrons (Brown 1971; Lin & Hudson 1976). Improved energy estimates for the thermal and nonthermal energy will help this situation.

While plasma temperatures may reach  $\sim 10$  to 15 MK in an average flare, temperatures in large flares can reach  $\gtrsim 30$  MK (e.g., Lin et al. 1981; Holman et al. 2003). At these temperatures, the thermal X-ray emission can be significant up to 30 keV or above. The highest temperatures generally occur during the solar flare impulsive phase seen in hard X-rays, when there is also nonthermal emission present. The low energy cutoff for nonthermal emission is not well known. Work done on some large, well-observed flares has suggested a cutoff energy in the 40 to 50 keV range (Lin & Johns 1993; Gan et al. 2002; Piana et al. 2003). Other researchers have noted that, for some flares, the nonthermal power law spectrum is dominant down to energies below 10 keV (Kane et al. 1992; Lin et al. 2001; Krucker et al. 2002). Thus both thermal and nonthermal emission may be present in the 10 to 30 keV range, and distinguishing between the two types of emission is difficult. This is important because it reflects directly on the amount of energy that is released in nonthermal electrons, and in the thermal plasma.

An accurate estimate of the thermal emission is needed to help make this distinction. This will require the use of multitemperature models for the thermal emission. Large flares tend to be morphologically complex, and we expect them to include a distribution of temperatures.

Our model uses the continuum and line emission from RHESSI spectra along with GOES data to obtain the differential emission measure (DEM) for a range of temperatures. We have a well-defined and proven method for combining data from different instruments to obtain the DEM and will use that method in the proposed study (McTiernan et al. 1999). The ability to obtain a reliable DEM will enable us to determine the energy present in the high temperature plasmas. In addition, we will be able to more accurately determine the energy contained in nonthermal electrons by obtaining better estimates of the low energy cutoff of nonthermal electrons.

The Reuven Ramaty High Energy Solar Spectroscopic Imager (RHESSI) will be the primary instrument used. RHESSI uses nine germanium detectors to observe solar X-rays and  $\gamma$ -rays in

the energy range from 3 keV to approximately 17 MeV. From RHESSI data, we can obtain spectra with better than 1 keV FWHM energy resolution (Lin et al. 2002; Smith et al. 2002). In solar flares, RHESSI can detect emission from plasmas with temperatures  $\gtrsim 10$  MK. RHESSI can detect both the thermal continuum and line emission (from Fe and Fe/Ni line complexes).

RHESSI is capable of imaging over its entire energy range through Fourier-transform methods using rotating modulation collimators. In front of each of the nine detectors, a pair of slit/slat grids separated by 1.55 meters act as a collimator with a 1-degree field of view. As the spacecraft rotates, the grids modulate the incident solar flux. Images of the photon source can be reconstructed from the modulated count spectrum, with an angular resolution that approaches 2 arcsec (Hurford et al. 2002).

RHESSI is extremely sensitive and it has detected flares with peak brightness ranging from GOES A level to greater than GOES X10. This large dynamic range is due to attenuators which move in front of the detectors when the photon count rate is high (and the detector live time is low). Since its launch in February 2002, RHESSI has observed more than 15000 flares, including more than 500 GOES X and M-class flares. We will use large flares for this study, and we should have a sample of at least 200 large M-class and X-class flares to work with.

The following sections explain the proposed research in more detail. In Section 2 we describe continuing research into the behavior of the  $\sim 6.7$  keV Fe line complex and the  $\sim 8$  keV Fe/Ni line complex observed by RHESSI, and how we will extend this research using multitemperature models.

In Section 3 we describe new research using RHESSI imaging spectroscopy to distinguish between thermal and nonthermal sources spatially. The RHESSI imaging spectroscopy will take advantage of new software that is available to calculate complex visibilities for RHESSI sources.

## 2. Fe and Fe/Ni Line Complex Ratios in Flares

Atomic physics presents a useful method of helping to determine the flare temperature distribution. In the solar flare spectrum  $\gtrsim 5$  keV, highly ionized iron (Fe) and nickel (Ni) generate numerous electronic excitation lines that cluster into two line complexes centered at  $\sim 6.7$  keV and  $\sim 8$  keV. (RHESSI has better than 1 keV FWHM spectral resolution at these energies, but cannot resolve individual lines within the complexes; thus the spectra show each line complex as a single “line” about 0.8 keV wide). The lines are most likely due to collisional excitation of ions by thermal electrons, with no significant contribution from photo-excitation by hard X-rays (Phillips 2004). The integrated flux in each of these two line complexes is strongly temperature-dependent, suggesting that they may be useful as diagnostics of the plasma temperature in flares. Also, the ratio is only very weakly dependent on the Fe and Ni abundance (Phillips 2004), and the line emissions do not suffer from ambiguity about thermal/nonthermal continuum representations. Since the lines span a limited energy range, we need only estimate the continuum flux under the lines, without

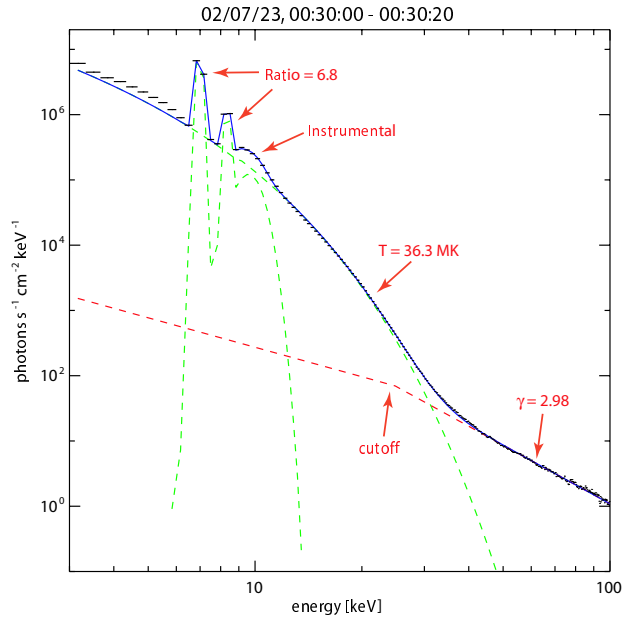


Fig. 1.— RHESSI spectral fit for an example photon spectrum of the 23 July 2002 X-class flare. The data (bars) are fit by a model spectrum (solid line) which is composed of a thermal continuum, a nonthermal continuum, and line emission (dashed lines). The temperature of the thermal component and the spectral index of the nonthermal component are denoted on the plot, and the position of the cutoff energy is marked. The Fe and Fe/Ni line complexes and a 10 keV instrumental “feature” are fit to gaussians.

requiring a thermal or nonthermal emission model, to obtain an accurate measurement of the line fluxes.

These two line complexes are visible in RHESSI flare spectra. Fig. 1 shows an example of this for the X-class flare that occurred on 23 July 2002. The 6.7 keV Fe complex is more easily excited at lower temperatures, and thus is seen in all but the smallest flares. The 8 keV Fe/Ni complex requires higher temperatures, and thus is seen with good statistics only in flares of GOES class M or higher. There is also a bump in the curve at approximately 10 keV that is currently believed to be L-shell emission from the tungsten included in the imager grids. Phillips (2004) predicted a specific correlation curve between the ratio of the fluxes in the two line complexes and the isothermal continuum temperature. Using RHESSI, we have measured these values and obtained empirical correlation curves. For the calculations of thermal line emission, version 5.1 of the CHIANTI software package was used; (Young et al. 2003; Dere et al. 1997).

Using RHESSI spectral data for a sample of large flares, we have approximately fit the 5–30 keV range with an isothermal continuum. Each line complex is fit to a gaussian shape. The isothermal approximation gives an emission-measure-averaged temperature and it is widely used

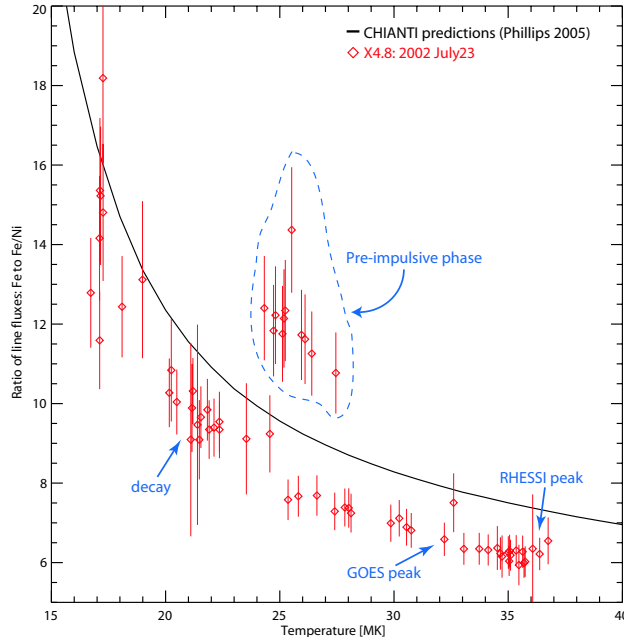


Fig. 2.— Theoretical curve (Phillips 2005) and measured data points for the ratio of the Fe line complex  $\sim 6.7$  keV and the Fe/Ni line complex  $\sim 8$  keV versus the isothermal continuum temperature.

historically and currently. This allows us to interpret our results in the context of many previous and current analyses. We know from RHESSI imaging that the line emission and the continuum thermal emission are cospatial. Measurements of the line ratio allow us to probe the same plasma that generates the thermal continuum independent of measurements of the continuum itself. Thus the line ratios provide another measure of the plasma temperature, independent of the continuum temperature measurement (Caspi & Lin 2007).

Our results verify that a strong temperature correlation does indeed exist. An example of this for the 23 July 2002 flare is shown in Fig. 2. With the exception of the early impulsive phase, the data for 23 July 2002 show a clear correlation between the line flux ratio and the isothermal temperature. During the early impulsive phase, there is no clear thermal continuum signature, and the spectra can be fit equally well by the standard isothermal continuum + power law *or* a broken power law down to 8 keV with no thermal continuum (Holman et al. 2003). In our research, we have found two flares which show this early impulsive behavior. Our proposed analysis may help solve this problem. Being able to differentiate between thermal and nonthermal emission using Fe and Fe/Ni line analysis and imaging spectroscopy would help resolve the ambiguity of the spectral fits during the early impulsive phase, and may provide clues to possible differences in the physical processes governing this period and the rest of the flare.

While all of the flares observed so far show a strong correlation of line ratio to continuum

temperature, the correlation is not often the same from flare to flare, and it does not necessarily match the theoretical curve. This behavior is not due to abundance variations. Since Fe emission contributes 85% or more of the flux in the Fe/Ni complex at typical flare temperatures, the line ratio is very weakly dependent on abundances. For example, doubling the Fe abundance would shift the ratio curve in Fig. 2 by less than 10%, a change smaller than the uncertainties in the observed ratio curve. This suggests that there is a multitemperature distribution of plasma. For a non-isothermal plasma the line flux ratio is dependent upon the temperature distribution. The differences in the ratio versus temperature behavior may help identify different temperature distributions between flares, and different temperature distributions during a flare.

The line ratio for the multitemperature model is easily calculated, and it constrains the differential emission measure by giving us the proportion of high temperature to low temperature plasma. We will find the DEM that best fits the continuum data, and then compare the line ratio calculated using that DEM to the observed value.

To obtain an estimate of the DEM, we will use an improved version of the method of McTiernan et al. (1999) and apply it to RHESSI and GOES data. The temperature response for GOES data has recently been updated by White et al. (2005) using the CHIANTI package. The use of GOES helps to stabilize the DEM solution at low temperature. In the DEM calculation, the temperature range is divided into bins and an emission measure is assigned to each bin. The amount of emission measure in the bins is then varied to minimize  $\chi^2$ . For the original SXT-BCS work, four bins were used for the range between 3 and 30 MK, since there were only five data points available. The histogram-DEM approximations typically fit the data well, and were improved by using the histogram-DEM as the starting point for a Maximum Entropy Method (MEM) calculation with 1 MK bins. This has been improved using two different methods: in one method the MEM technique is replaced with a 1-dimensional version of the pixon technique used successfully for Yohkoh HXT and RHESSI imaging (Metcalf et al. 1996). Fig. 3 shows the result for a test of the pixon-DEM code. A trial DEM with the form of a power law with a hump at 18 MK was created and integrated over the temperature responses of RHESSI and GOES to get a simulated “observed” spectrum. Poisson noise was added to the spectrum, and the resulting trial dataset was then input into the DEM recovery calculation. This calculation was repeated a large number of times in a Monte Carlo calculation, to obtain uncertainties for the recovered DEM.

In the top panel of the figure, the dashed line represents the input DEM. The histogram represents the recovered DEM. The bottom panel shows the residual in each energy channel, divided by the uncertainty in the counts for the spectrum. The average reduced  $\chi^2$  value for this test was approximately 2.0, in spite of the fact that the bump in the input spectrum is not fit very well. This is a reflection of the temperature resolution of the detector; RHESSI is not a narrow-band instrument such as SOHO/CDS, and any narrow feature will have a width of a few MK. Solutions for this sort of inversion problem are not unique. For example, an emission measure distribution with many sharp features will be represented as a smooth function. This is still much better than an isothermal approximation. The test with the narrow hump is a worst-case scenario; broad features

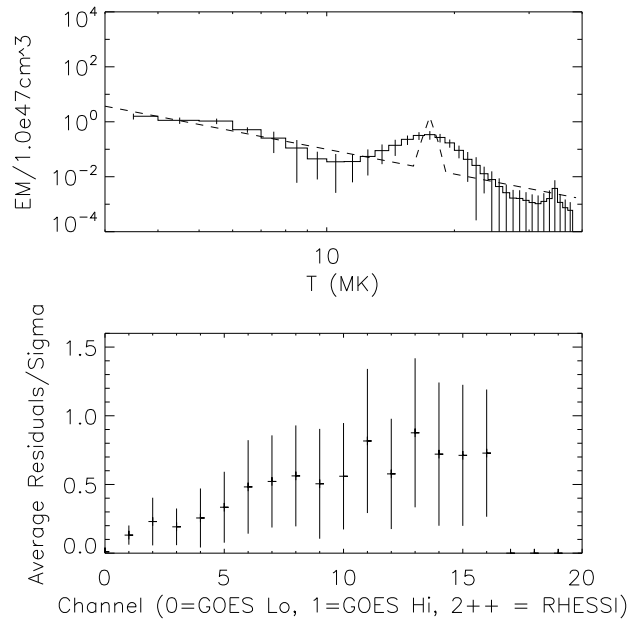


Fig. 3.— Test of the DEM method. Top: The dashed line is the input DEM and histogram with error bars represents the recovered DEM. Bottom: The average of the absolute value of the residuals divided by the uncertainties in the input data, which for this test were approximately 2%.

in the DEM are fit much better.

We have also developed a method that fits DEM to an N-element power law. The temperature range is divided into a number of smaller temperature bands, and the DEM is represented by a different power law in each of these bands. This function is required to be continuous at the edges of each of the small temperature bands. For the initial calculation, a single power law is used for the whole temperature range. Next, this range is split into two bands and the fit is performed. A reduced  $\chi^2$  is calculated:

$$\chi^2 = (N - 2N_{pl})^{-1} \sum (c_{model} - c_{obs})^2 / \sigma^2, \quad (1)$$

where  $c_{model}$  are the photon count rates expected from the DEM model,  $c_{obs}$  are the observed count rates,  $\sigma$  are the uncertainties in the count rates,  $N$  is the total number of data points, and  $N_{pl}$  is the number of power law components (equivalent to the number of smaller temperature bands). If this quantity decreases, then this DEM is saved, the full range is split into three bands, and the fit is performed again. The process continues until a minimum value of reduced  $\chi^2$  reached. For each step, a simulated annealing fit procedure (Press et al. (1986)) is used for the fit. We will use both methods to get estimates of the DEM and require that the results are consistent before further analysis. Tests of trial DEMs with a number of different functional forms have given us confidence that the DEM for a flare in the 5 to 30 MK range can be reliably recovered using this combination of GOES and RHESSI.

Nonthermal emission will be included in form of a power law photon spectrum with a low energy cutoff. The process will be as follows: The nonthermal spectrum obtained by fitting high energy (above 40 or 50 keV) emission is extended down to a low energy cutoff value, and the spectrum below the cutoff is assigned a power law spectral index of  $\gamma = -1.4$ , which is the expected value for bremsstrahlung emission from an electron distribution with a sharp cutoff. For low energies, this nonthermal spectrum does not account for all of the observed emission (See, for example, Fig. 1). The DEM is then fit using the remaining emission. This process is repeated for all cutoffs above 5 keV.

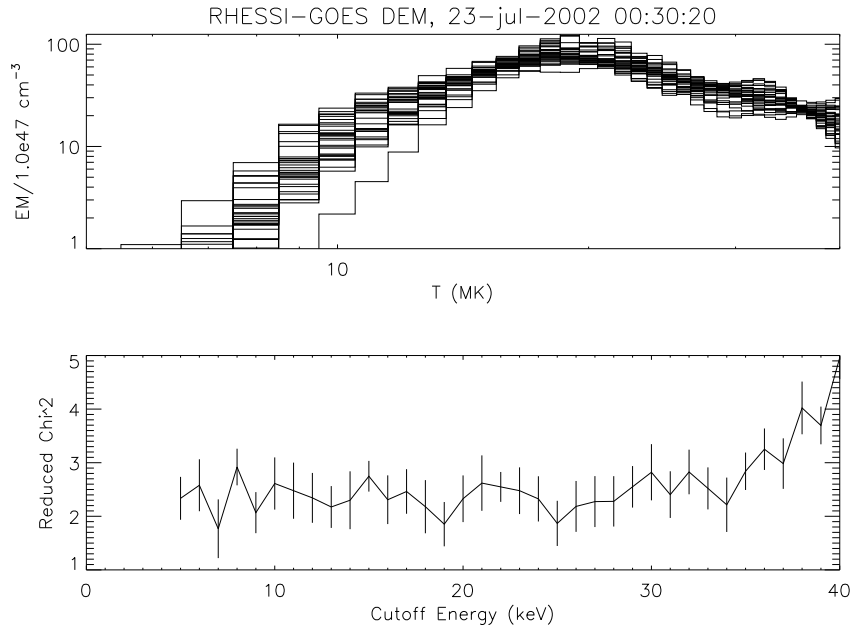


Fig. 4.— Test of the DEM plus nonthermal method. Top: A superposition of the DEM calculated for cutoff energies from 5 to 40 keV for the 23-jul-2002 flare. Bottom: the reduced  $\chi^2$  goodness of fit parameter as a function of cutoff energy. The error bars are obtained from a Monte Carlo calculation.

The low energy cutoff for nonthermal electrons is often not well constrained when the thermal and nonthermal spectra overlap. Using a DEM fit for the thermal spectrum results in a large range of possible cutoff energies. A demonstration of this from preliminary calculations is shown in Fig. 4. The top panel is a superposition of the DEM calculated for cutoff energies from 5 to 40 keV for the 23-jul-2002 flare. The bottom panel shows the value of the reduced  $\chi^2$  as a function of cutoff energy. For low energies there is no difference in the goodness of fit. Above approximately 37 keV the data is not fit well, and this gives us an upper limit to the cutoff energy. This is also clear from Fig. 1; thermal emission is so dominant that moving the cutoff energy to low energy will have a negligible effect on any derived thermal parameters. The break cannot be moved to a high energy however; doing so would cause an unobserved dip in the spectrum. Because of this effect, what

is measured is an upper limit to the cutoff energy, and a lower limit to the energy in nonthermal electrons.

For flares in which the thermal component is not so dominant, this may not be the case. Fig. 5 shows the same calculation for a flare which occurred on 26-feb-2002. This flare had less thermal emission; it was a C9.6 in GOES class, but had a substantial nonthermal component including  $\gamma$ -ray emission. For this flare, the DEM plus nonthermal model only fits well between 22 and 26 keV, giving a relatively narrow range of possible cutoff energies. We expect that most flares will lie between the two extremes, resulting in a high uncertainty ( $\gtrsim 10$  keV in the cutoff energy, and a correspondingly large uncertainty (and often only a lower limit) in the energy of nonthermal electrons. But even with this large uncertainty, this measurement is superior to previous estimates that simply assumed a constant value of the cutoff for all flares, or used an isothermal approximation for the thermal emission.

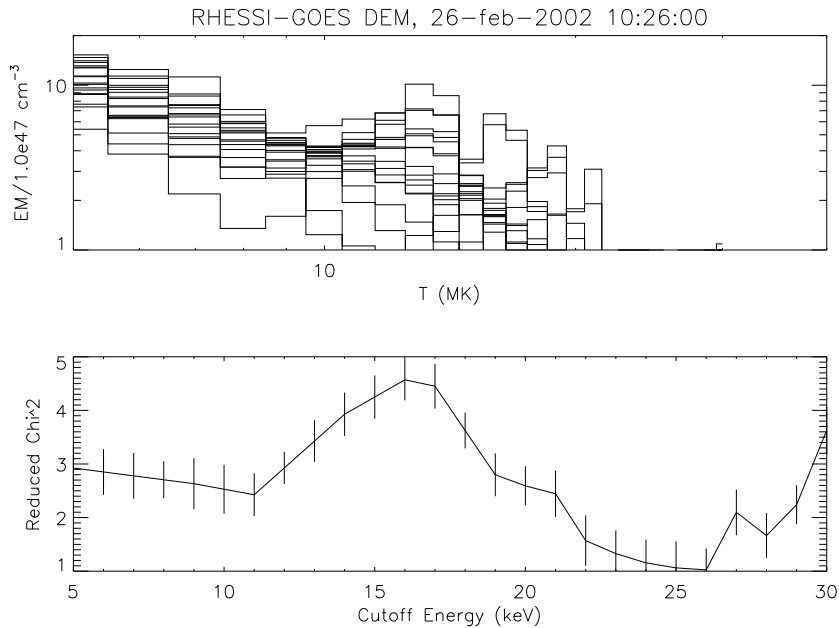


Fig. 5.— Test of the DEM plus nonthermal method. Top: A superposition of the DEM calculated for cutoff energies from 5 to 30 keV for the 26-feb-2002 flare. Bottom: the reduced  $\chi^2$  goodness of fit parameter as a function of cutoff energy. The error bars are obtained from a Monte Carlo calculation.

For this work, good calibration of the spectral response of the RHESSI detectors is essential. For this research we will always use the latest RHESSI calibration data and the latest version of the CHIANTI software package (currently version 5.2) to obtain our results. There are some known calibration issues that affect RHESSI data, and our research can also help to provide information about these issues. For example, spectra obtained from the individual detectors on RHESSI may differ by 5 to 10%. To overcome this, we will analyze data from individual detectors, and compare

their results. There are uncertainties in the estimated effect of the attenuators at the lowest energies ( $\lesssim 10$  keV). Since we will be comparing spectra for different attenuator states in individual flares, we may be able to improve the corrections for attenuator states. Also, there are artifacts in the spectra which are not yet accounted for in the RHESSI software package, such as the 10 keV “line feature” shown in Fig. 1. Currently, these features are empirically fit to account for their effects. Despite these calibration issues, we are confident the empirical corrections are good and that our results will be robust.

We will work with as large a sample of flares as possible, concentrating on X-class and high M-class flares, for good statistics. We expect to analyze approximately 200 flares. For each flare, we will:

- Fit the continuum emission to a DEM model including a nonthermal component, and obtain an estimate for the low energy cutoff for nonthermal electrons. We know of no other work that has obtained this information from a large ( $\gtrsim 100$ ) number of flares.
- Take the empirically derived DEM and recalculate the expected line flux ratios, which we will then compare to the observed line flux ratios. The line complexes will provide us with an independent constraint for the DEM, and perhaps reduce the uncertainty in the cutoff energy.

**Note About Fe, Ni Abundances:** As mentioned previously, the ratio calculation is not strongly dependent on abundances. Thus, even though we will carry out the calculations for different values of the abundances, it will most likely be impossible to discern the effect of differences in the abundances. This is in contrast to work which uses the equivalent width of the line complexes, which is strongly dependent on the ionic abundances (Phillips et al. 2006).

### 3. Imaging Spectroscopy

RHESSI imaging spectroscopy offers the opportunity to distinguish spatially between thermal and nonthermal sources. RHESSI data can be used for source-based imaging spectroscopy. This is not a pixel-to-pixel comparison as is often done for TRACE or EIT, but rather is a spectrum obtained for different source regions (see e.g., Emslie et al. 2003). The standard procedure is to create images in different energy bands, draw a box around a certain region of each image, and obtain a spectrum from the total of the observed photons in the box for each image. Since the observed count spectrum is a product of the incident photon spectrum and the detector response matrix, the photon spectrum is obtained from the count spectrum by either inverting the detector response matrix or by forward-fitting a model.

Fig. 6 shows RHESSI images of the X-flare on 23 July 2002. The left hand image shows the emission in the 6.3 to 7.3 keV band that contains the Fe line complex discussed in the previous

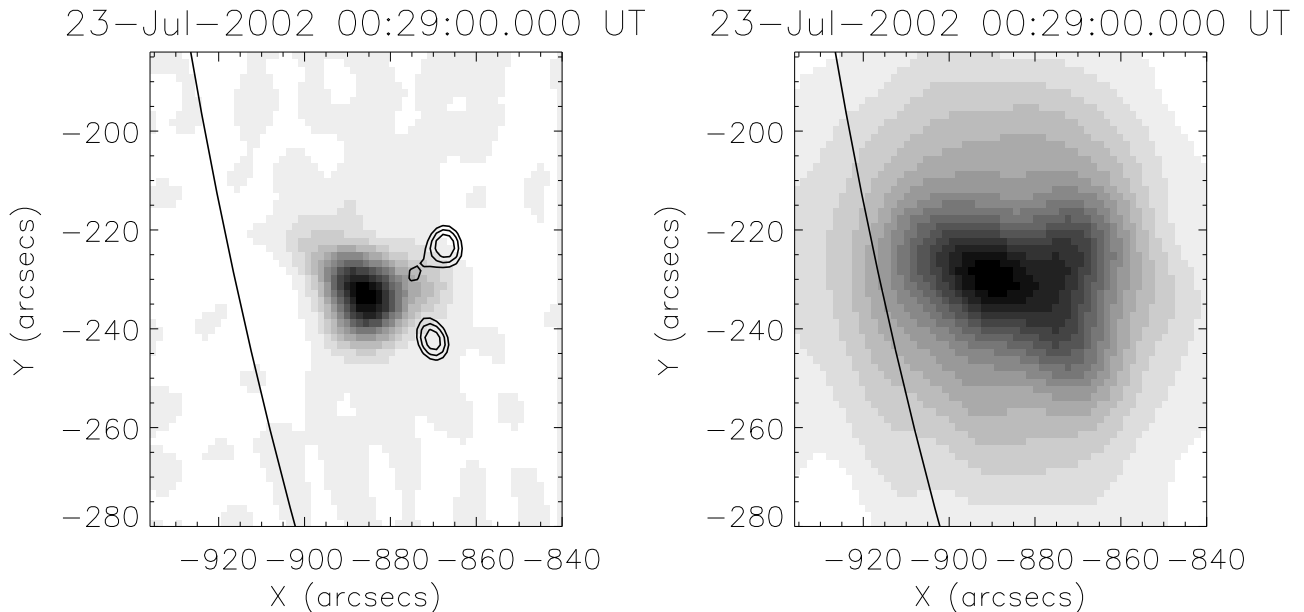


Fig. 6.— Left: Image of the 23 July 2002 solar flare in the 6.3 to 7.3 keV energy band. The contours show the emission in the 50 to 100 keV energy band. Right: The RHESSI image in the 36 to 40 keV band, which has components for both thermal and nonthermal sources.

section. The contours show what we expect to be the nonthermal emission from loop footpoints, with the low energy thermal source, which is believed to be high in the corona, between the footpoints (Emslie et al. 2003). The image on the right is the image in the 36 to 40 keV band, where the sources are not as spatially distinct.

The spectra for the thermal and nonthermal sources for the time interval used in Fig. 1 are shown in Fig 7. Here the dashed line represents the thermal spectrum, and the solid line represents the nonthermal spectrum (actually the sum of the two footpoint spectra). These spectra were obtained as explained above; images were created in 1 keV energy bands, boxes were drawn around the sources, and the photon counts inside the boxes were totaled and passed into the OSPEX software package that is used for RHESSI spectroscopy<sup>1</sup>.

The thermal source shows a bump in the 6 to 7 keV channel that corresponds to the Fe line complex, but the Fe/Ni line complex is not very noticeable with this spectral resolution. The temperature measurement is similar to that obtained in Fig. 1. For the nonthermal spectrum, the break energy is higher, at 36 keV, and the spectrum above the break is somewhat steeper.

There are some complications involved in this method. For large flares, the image properties

---

<sup>1</sup>For a description of OSPEX: [http://hesperia.gsfc.nasa.gov/ssw/packages/spex/doc/ospex\\_explanation.htm](http://hesperia.gsfc.nasa.gov/ssw/packages/spex/doc/ospex_explanation.htm)

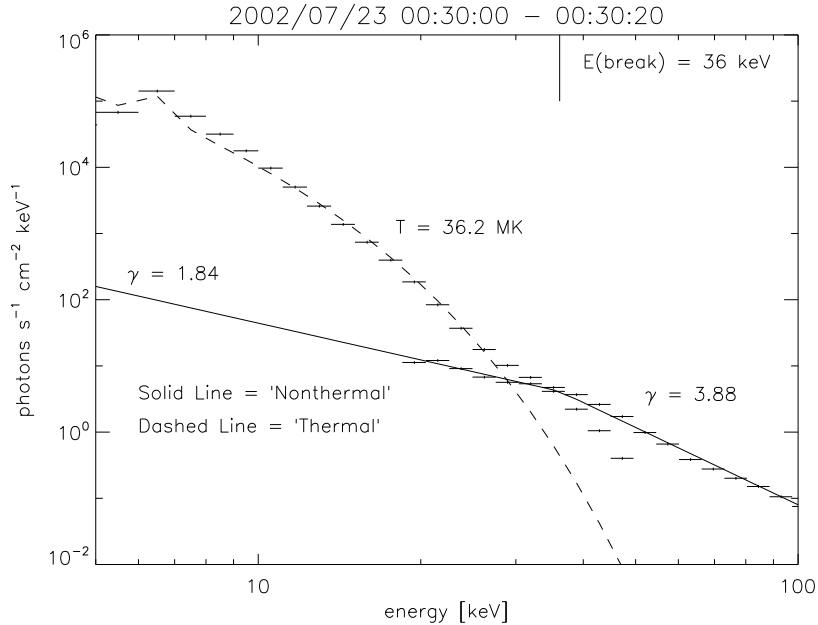


Fig. 7.— Spectra for the thermal and nonthermal sources for the 23-Jul-2002 flare. The dashed line is the spectrum of the thermal source, and the solid line is the spectrum of the two nonthermal footpoints combined.

at low energy are strongly affected by the attenuators that are moved in front of the detectors. The attenuators decrease the number of low energy photons that are observed, and for a low-energy image, many of the detected counts are actually due to photons with energy  $\sim 10$  keV higher. (This occurs when an incident photon excites a K-shell transition in the detector and the subsequent  $\sim 10$  keV K-shell photon escapes from the detector. We refer to this as “K-escape”.)

RHESSI images are not corrected for this effect, and the number of “photons” in the image at a given energy is calculated making the assumption that the spectral response matrix is diagonal, i.e. that all of the counts observed in a given energy range are due to photons with incident energies in that energy range. When the attenuators are in, this is not a good approximation and there are significant off-diagonal components in the response matrix. Using OSPEX, we can correct for these off-diagonal elements during the spectroscopic analysis. Specifically, we convert the image photon fluxes back into counts by multiplying the photon spectra by the diagonal response matrix. The resulting count spectrum is then fed into OSPEX and the full detector response, including off-diagonal elements, is applied.

There are other difficult-to-quantify uncertainties in this calculation. The choice of which pixels in each image are assigned to which source is not always well defined. This is a particular problem in the energy range where both types of emission are important (e.g. 20 to 40 keV) and the sources may be difficult to separate, as shown on the right hand side of Fig. 7. Also, with the exception of

the PIXON algorithm, the RHESSI imaging algorithms do not return uncertainties, so there is no known uncertainty in the photon flux in an image. The error bars in the spectral plot are rough estimates, based on an estimated 5% systematic error. In addition, the complications discussed in the previous section (e.g., uncertainties in the attenuator effects and uncertain detector-to-detector calibration) are present.

Some of these problems, in particular the possible confusion between sources and the lack of uncertainties in the imaging process, can be addressed by using new RHESSI software that calculates source visibilities (Hurford et al. 2005)<sup>2</sup>.

A visibility is a complex number that corresponds to a measurement of one Fourier component of the source brightness at a given spatial frequency. The RHESSI software now features a visibility-based forward-fitting method in which the visibilities are used to fit a given number of sources. Each source in an image is modeled by a circular gaussian and the process obtains the position, width and photon flux in the sources by minimizing  $\chi^2$ . One benefit of this process is that it returns an error estimate for each parameter, based on photon statistics. A disadvantage of this process is that it may not give good results for oddly shaped sources. Currently fitting curved and elliptical sources is possible, but only for single sources. When multiple sources become feasible, we will test this option.

For imaging spectroscopy, the visibilities are calculated for different energy bands and used to obtain the source photon fluxes. The calculation of the visibilities also assumes a diagonal spectral response (i.e. that the observed energy of a photon count is equal to the energy of the incident photon). The photon fluxes obtained from the visibilities are converted back into counts by multiplying the the source photon flux by the diagonal response and the result is passed into OSPEX. As previously discussed, this accounts for the full response matrix, including the off-diagonal elements. The final product is a fit photon spectrum for each source. For each solar flare that is analyzed, we will use both methods: the traditional imaging spectroscopy and the visibility-based forward fitting process.

RHESSI imaging spectroscopy gives us accurate measurements which can be used for temperature and emission measure calculation. In some cases, TRACE data can be combined with RHESSI data for the thermal source to obtain the DEM. Recent research (Phillips et al. 2005; Warren & Reeves 2001) has shown that TRACE has a response to high temperature (10 to 20 MK) plasma in the 171 and 195 Angstrom filters. As shown in the previous section, we have a method of recovering the differential emission measure using data from multiple instruments. This was used by McTiernan et al. (1999) for solar flares using Yohkoh SXT and BCS data, and has more recently been used by McTiernan & Klimchuk (2003) to recover the quiet-sun DEM using RHESSI and GOES12-SXI data.

We will analyze the spatially distinct sources that can be found in well-observed flares. The

---

<sup>2</sup>Also: <http://sprg.ssl.berkeley.edu/~ghurford/Visibility%20Routines/VisibilityGuide.pdf>

first task for this work will be to obtain a good sample of solar flares. The requirements will be as follows: (1) The flares need to be relatively large, probably GOES class M or higher, to insure that there are enough photons available for imaging spectroscopy. (2) The morphology of the flare must be such that the soft thermal and hard nonthermal sources can be identified, allowing independent spectral calculations. For this purpose, we also will use images from other instruments, such as TRACE, EIT, or MDI, which will allow us to locate the different sources with respect to the magnetic configuration of the flare’s parent active region. We expect to find 10 to 20 flares based on these criteria.

Once a representative sample of flares has been found, we will:

- Create RHESSI images and visibilities in 1 keV energy bands for the energy range above 5 keV. We will use the images and the visibilities to perform imaging spectroscopy and compare the results of the different methods.
- Establish that the “thermal” source is indeed dominated by thermal emission by checking for the presence of the Fe line complex in spectra from that source. From the work described in the previous section, we will have a good idea of how much line emission to expect from a thermal source.
- Use these images to obtain isothermal temperatures and emission measures, and also the DEM. If good data are available from TRACE, we will include those data. This will give us a good estimate of the energy in the thermal plasma. We will also be able to get a good estimate for the energy “missed” by RHESSI by comparing the DEM for multi-instrument fits with the DEM obtained using only RHESSI.
- Fit spectra to the nonthermal sources. From this we get a good estimate of the balance of energy between the thermal and nonthermal electrons.
- Compare these results to those obtained using non-imaging spectroscopy techniques.

#### 4. Impact of Proposed Work

The research that has been outlined in this proposal is significant in a number of ways:

- Quantitative estimates of the energy released in solar flares are important. Good energy estimates help researchers to develop and test theories of plasma heating and particle acceleration in flares. Also, good energy estimates are needed for research that compares flare energy to CME energy and to the energy of active region magnetic fields. Adapting the multitemperature fitting process will improve these estimates.
- Techniques for combining spectral data from different instruments in a quantitative manner are rare, but are essential for current missions. This work will also be applicable to future

missions; in particular, the multi-instrument techniques can easily be adapted for use with SOLAR-B/XRT data and SDO/AIA data.

## 5. Relevance of Proposed Work to the NASA Programs/Objectives

This work is directly related to the acceleration of charged particles, and also to coronal heating processes; thus it is relevant to NASA Science Question: “How and why does the Sun vary?” and NASA Research Objective: “Understand the fundamental physical processes of the space environment from the Sun to Earth, to other planets, and beyond to the interstellar medium.”

## 6. Work Plan and Personnel

Dr. James McTiernan, the Principal Investigator for this project, is an Associate Research Physicist at UCB-SSL. He is a member of the RHESSI team and has experience with spectral deconvolution, image processing and DEM calculations.

Mr. Amir Caspi is a Ph.D. student in the Physics Department at UCB. The current proposal is an extension of Mr. Caspi’s research using the ratio of line complexes for temperature diagnostics.

For the first year of the research, we will concentrate on the characterization of the Fe and Fe/Ni line complex spectra and verification of the DEM calculation process, for spatially integrated spectra. During the following years, we will concentrate on the imaging spectroscopy for flares. By the start time of the proposed work, the imaging spectroscopy capabilities included in the RHESSI software will be more advanced than are now available. When we are satisfied that we have good source-based imaging spectroscopy data available, we will use these data, along with data from other instruments to obtain the multi-instrument DEM.

## 7. References

### REFERENCES

- Brown, J. C. 1971, *Sol. Phys.*, 18, 489
- Caspi, A. & Lin, R. P. 2006, *ApJ*, in preparation
- Dere, K. P. et al. 1997, *A&AS*, 125, 149
- Emslie, A. G., Kontar, E. P., Krucker, S. & Lin, R. P. 2003, *ApJ*, 595, L107
- Gan, W. Q., Li, Y. P., Chang, J. & McTiernan, J. M. 2002, *Sol. Phys.*, 207, 137
- Holman, G. D., Sui, L., Schwartz, R. A. & Emslie, A. G. 2003, *ApJ*, 595, L97
- Hurford, G. J. et al. 2002, *Sol. Phys.*, 210, 61
- Hurford, G. J., Schmahl, E. J. & Schwartz, R. A. 2005, *Eos Trans. AGU 86(18)*, Jt. Assem. Suppl., Abstract #SP21A-12
- Lin, R. P. & Johns, C. M. 1993, *ApJ*, 417, L53
- Kane, S. R. et al. 1992, *ApJ*, 390, 687
- Krucker, S. et al. 2002, *Sol. Phys.*, 210, 445
- Lin, R. P. & Hudson, H. S. 1976, *Sol. Phys.*, 50, 153
- Lin, R. P., Schwartz, R. A., Pelling, R. M. & Hurley, K. C. 1981, *ApJ*, 251, 109
- Lin, R. P., Feffer, P. T. & Schwartz, R. A. 2001, *ApJ*, 557, L125
- Lin, R. P. et al. 2002, *Sol. Phys.*, 210, 3
- McTiernan, J. M., Fisher, G. H. & Li P. 1999, *ApJ*, 514, 472
- McTiernan, J. M. & Klimchuk, J. A. 2003, *Eos Trans. AGU 84(46)*, Fall Meet. Suppl., Abstract #SH21B-0162
- Metcalf, T. R., Hudson, H. S., Kosugi, T., Puetter, R. C. & Pina, R. K. 1996 *ApJ*, 466, 585
- Phillips, K. J. H. 2004, *ApJ*, 605, 921
- Phillips, K. J. H., Chifor, C. & Landi, E. 2005, *ApJ*, 626, 1110
- Phillips, K. J. H. 2005, private communication
- Phillips, K. J. H., Chifor, C. & Dennis, B. R. 2006, *ApJ*, 647, 1480

Piana, M. et al. 2003, *ApJ*, 595, L127

Press, et al. 1988, “Numerical Recipes”, Cambridge University Press.

Smith, D. M. et al. 2002, *Sol. Phys.*, 210, 33

Warren, H. P. & Reeves, K. K. 2001, *ApJ*, 554, L103

White, S. M., Thomas, R. J. & Schwartz, R. A. 2005, *Sol. Phys.*, 227, 231

Young, P. R. et al. 2003, *ApJS*, 144, 135

## 8. Biographical Sketch

**James M. McTiernan**

**Title:**

Associate Research Physicist

**Address & Telephone:**

Space Sciences Laboratory

University of California

Berkeley, CA 94720

(510)643-9246

email: jimmm@ssl.berkeley.edu, jmctiernan@solar.stanford.edu

**Education** 1981: B. A. Physics, Rutgers University, New Brunswick, NJ.

1989: Ph. D. Applied Physics, Stanford University, Stanford, CA.

**Career Summary:**

1981-1989: Graduate Research Assistant, Stanford University, Stanford, CA.

1989-present: Assistant/Associate Research Physicist, Space Sciences Laboratory, University of California, Berkeley, CA.

**Scientific, Technical, and Management performance on relevant prior research efforts:**

Dr. McTiernan developed the Solarsoft version of the Optimization NLFFF code, and is responsible for upgrades and maintenance. As SOC scientist for the RHESSI project, Dr. McTiernan is responsible for the creation of the online database, and quicklook data, and the maintenance of the part of the RHESSI software package that pertains to these processes.

**Selected Publications:**

J. M. McTiernan, G. H. Fisher & P. Li, “The Solar Flare Soft X-Ray Differential Emission Measure and the Neupert Effect at Different Temperatures”, *ApJ*514, 472, (1999).

J. T. Mariska & J. M. McTiernan, “Hard and Soft X-Ray Observations of Occulted and Nonocculted Solar Limb Flares”, *ApJ*514, 484, (1999).

V. Petrosian, T. Q. Donaghy & J. M. McTiernan, “Loop Top Hard X-Ray Emission in Solar Flares: Images and Statistics”, *ApJ*569, 469, (2002)

G. Trottet, R. A. Schwartz, K. Hurley, J. M. McTiernan, S. R. Kane, N. Vilmer, “Stereoscopic observations of the giant hard X-ray/gamma-ray solar flare on 1991 June 30 at 0255 UT”, *å*403 1157, (2003).

K.-L.Klein, R. A. Schwartz, J. M. McTiernan, G. Trottet, A. Klassen, A. Lecacheux, “An upper limit of the number and energy of electrons accelerated at an extended coronal shock wave”, *Å407* 317, (2003).

W. P. Abbett, Z. Mikic, J. A. Linker, J. M. McTiernan, T. Magara, and G. H. Fisher, “The Photospheric Boundary of Sun-to-Earth Coupled Models”, *JASTP*, (2004).

S. R. Kane, J. M. McTiernan, K. Hurley, “Multispacecraft observations of the hard X-ray emission from the giant solar flare on 2003 November 4”, *Å433*, 1133 (2005).

C .J. Schrijver, M. L. Derosa, T. R. Metcalf, Y. Liu, J. M. McTiernan, S. Rgnier, G. Valori, M. S. Wheatland, T. Wiegelmann, “Nonlinear Force-Free Modeling of Coronal Magnetic Fields Part I: A Quantitative Comparison of Methods” *Solar Physics* 235, 161 (2006).

## 9. Current and Pending Support

James McTiernan, Current Support:

THEMIS mission, NASA contract NAS5-02099 (50%)

RHESSI mission, NASA contract NAS5-98033 (25%)

NASA Sun-Earth Connection Theory Grant NASA contract NNG05GI44G (25%)

Pending support:

NSF/SHINE grant: "Driving Solar MHD simulations with Vector Magnetogram Sequences" P.I.: Dana Loncope (Montana State University). (30%, for the first two years of this proposed work)

NASA Heliospheric GI Proposal: "Full-Disk Solar EUV Spectroscopy with CHIPS", PI: M. Hurwitz

NASA Heliospheric GI Proposal: "Statistical Studies of Coronal Hard X-ray Sources" PI: S. Krucker

## 10. Budget Justification

This work will mostly be carried out by Amir Caspi, a graduate student at UCB. The PI, James McTiernan, will supervise this work and provide data analysis software necessary for the DEM calculations, and also for Imaging Spectroscopy. We are requesting 5.5 months salary per year for Mr. Caspi, and 2 months per year for Dr. McTiernan. Also included are costs for travel to one meeting per year, publication costs, and costs for administration of computer resources.

### Summary of Personnel and Work Efforts:

Personnel	Year 1 (WY)	Year 2 (WY)	Year 3 (WY)
PI: James McTiernan	0.16	0.16	0.16
Grad Student: Mr. Amir Caspi	0.45	0.45	0.45

### Budget Details:

	Year 1	Year 2	Year 3
Travel:			
5-day RT to East Coast Conf.	\$1680	\$1680	\$1680
Airfare	\$600	\$600	\$600
Lodging/Meals	\$171 per day	\$171 per day	\$171 per day
Car Rental	\$45 per day	\$45 per day	\$45 per day
Other:			
Datalab System Admin	\$1230	\$1264	\$1299
Publication	\$1000	\$1000	\$1000

### Facilities and Equipment

For this research, we will use facilities and equipment currently available at SSL. No new equipment will be purchased.